



Revealing the impacts of climate change on mountainous catchments through high-resolution modelling

Jorge Sebastián Moraga^{a,*}, Nadav Peleg^{a,b}, Simone Fatichi^c, Peter Molnar^a, Paolo Burlando^a

^a Institute of Environmental Engineering, ETH Zurich, Zurich, Switzerland

^b Institute of Earth Surface Dynamics, University of Lausanne, Lausanne, Switzerland

^c Department of Civil and Environmental Engineering, National University of Singapore, Singapore

ARTICLE INFO

This manuscript was handled by Emmanouil Anagnostou, Editor-in-Chief, with the assistance of Qiang Dai, Associate Editor

Keywords:

Catchment modelling
Climate change impacts
Weather generator
Distributed hydrological model
Streamflow extremes
Hydrological response

ABSTRACT

Mountainous catchments cover a broad range of elevations and their response to a warming climate is expected to vary significantly in space. Nevertheless, studies on climate change impacts typically examine the changes in flow statistics only at the catchment outlet. In this study, we instead demonstrate the high variability of the hydrological response to climate change at the sub-catchment scale, investigating in detail the contribution of all components of the hydrological cycle in two mountainous catchments (Thur and Kleine Emme) in the Swiss Alps. The analysis was conducted with a two-dimensional weather generator model that simulated gridded climate variables at an hourly and 2-km resolution until the end of the 21st century for the RCP8.5 emission scenario. The climate ensemble was used as input into a distributed hydrological model to estimate the changes in hydrological processes at 100-m and hourly resolutions. Climate models show that precipitation intensifies during winter but weakens during summer in the order of ± 5 –10% toward the end of the century. Temperature will rise by up to 4°C, leading to a 50% reduction in snowmelt, 10% increase in evapotranspiration, and shift in precipitation type from snowfall to rainfall. As a result, streamflow is projected to increase by 40% in winter but decrease by 20% to 40% during summer, with winter floods becoming more frequent. The changes to streamflow (mean and extreme low and high flows) at the sub-catchments show a strong dependency with elevation. In contrast to the small changes projected at the outlet of the catchments, streamflow shows a reduction at higher elevations (up to –20% change in mean streamflow for sub-catchments at elevations exceeding 1400 m) and an increase at lower elevations (up to +5% for Kleine Emme and +20% for the Thur at elevations below 600 m). These impacts are tied to the changes in precipitation, as well as changes in snowmelt (at high elevation) and evapotranspiration (at low elevation). The results reveal the causes and diversity of hydrological response to climate change, emphasizing the importance of investigating the distributed impacts of climate change in mountainous environments.

1. Introduction

Global warming is affecting hydrological processes in many regions and across various space–time scales. Mountainous catchments are no exception: a diminishing snow cover and glacier retreat (Blanc and Schaedler, 2014; Beniston et al., 2018; Bultot et al., 1994; Etter et al., 2017; Jenicek et al., 2018; Jörg-Hess et al., 2015), and changes in intense meteorological events, such as prolonged droughts and intensification of extreme precipitation (Ban et al., 2015; Bao et al., 2017; Fischer et al., 2015; Lenderink et al., 2017; Peleg et al., 2018; Westra et al., 2014), suggest that their hydrological cycle could undergo significant alterations. Among the expected consequences are increased

hazards such as floods, low flows, landslides, or debris flows (Brunner et al., 2019; Floriancic et al., 2020; Gariano and Guzzetti, 2016; Hirschberg et al., 2021; Kos et al., 2016; Scheidl et al., 2020), which in turn can lead to serious impacts on infrastructure, irrigation demand, hydropower production, and tourism, with significant economic consequences (Abegg et al., 2007; Zubler et al., 2015; Savelsberg et al., 2018; Weingartner et al., 2013). Adapting to these changes and mitigating their effects requires modelling the hydrological response of mountainous catchments at scales appropriate for the involved hydrological processes and suitable to represent the highly heterogeneous mountainous topography. This implies spatial resolutions in the order of kilometers and time steps of hours or less (e.g., Mastrotheodoros et al.,

* Corresponding author.

E-mail address: moraga@ifu.baug.ethz.ch (J.S. Moraga).

<https://doi.org/10.1016/j.jhydrol.2021.126806>

Received 19 February 2021; Received in revised form 3 June 2021; Accepted 6 August 2021

Available online 13 August 2021

0022-1694/© 2021 The Author(s).

Published by Elsevier B.V. This is an open access article under the CC BY-NC-ND license

(<http://creativecommons.org/licenses/by-nc-nd/4.0/>).

2020). Achieving this level of detail is challenging, as modelling at these fine scales demands substantial computational resources and large amounts of high-resolution observations to calibrate and validate models. Moreover, a changing climate means that relations between hydro-meteorological variables in the past may no longer hold in the future, questioning the validity of data-driven relations in predicting future behavior (Milly et al., 2008). Hence, the appeal of physically-based distributed models for estimating the hydrological response to a changing climate.

Physically-based (also known as process-based) hydrological models are suited to estimate the hydrological response of catchments under changing climatic forcing (Faticchi et al., 2016b). With little to no parameter calibration, they capture the dynamics of atmosphere-land interactions and reproduce them, in theory, for any catchment or climatic input. While spatially lumped hydrological models cannot reproduce the diversity of responses within the catchments, distributed models can provide a meaningful cause-and-effect association throughout the catchment (Mascaro et al., 2015). By forcing them with climate variables from climate models, physically-based hydrological models can be used to compute the impact of global warming on other hydrological variables besides streamflow, such as soil moisture, snowmelt, and evapotranspiration (ET). This approach has provided valuable insights into, for example, the role of storm structure in runoff generation (Paschalis et al., 2014), the sensitivity of climate change response to the overall soil permeability of the catchment (Camici et al., 2017), the relation between runoff and elevation and its meaning for future hydropower production (Faticchi et al., 2015), and the detailed understanding of the eco-hydrological response to changing climate conditions (Mastrotheodoros et al., 2020).

The effects of global warming on individual climate variables are typically inferred from General Circulation Models (GCM) and Regional Climate Models (RCM), albeit at scales that make them unsuitable to study most hydrological processes, in particular at the scale that controls the response of mountainous catchments (Faticchi et al., 2013; Mateo et al., 2017). Therefore, downscaling of climate variables to suitable space-time scales is required (Smiatek and Kunstmann, 2019). This can be accomplished using stochastic weather generators (WG), as alternatives to other dynamic or statistical methods (see review papers by Fowler et al., 2007; Maraun et al., 2010; Trzaska and Schnarr, 2014). Using historical observations and GCM/RCM outputs, WGs combine physical relationships among climatic variables and a stochastic approach to generate synthetic time series that reproduce the statistics of the observed data, and once suitably re-parameterized, simulate climate variables for future periods (e.g., Faticchi et al., 2011; Fowler et al., 2007; Peleg et al., 2017; Semenov & Barrow, 1997; Wilks & Wilby, 1999; Wheeler et al., 2005). Most WGs simulate climate variables at either the point scale (Faticchi et al., 2011; Parket et al., 2018) or at multiple sites (Bordoy and Burlando, 2014; Keller et al., 2017; Keller et al., 2015). In recent years, two-dimensional WGs were developed, such as STORM (Singer et al., 2018; Singer and Michaelides, 2017) and AWE-GEN-2d (Peleg et al., 2017), capable of downscaling gridded climate variables. Besides downscaling, the purpose of WGs is to produce climatic ensembles, i.e. multiple realizations characterizing the climate conditions, which allows probabilistic analysis of change and quantification of uncertainty.

The present study aims to quantify the effects of climate change on hydrological processes in mountainous catchments and to assess how the hydrological response varies in space. We hypothesize that the magnitude, and perhaps even the direction (signal), of change will be related to elevation, because some of the hydrological components that contribute to streamflow (e.g. evapotranspiration or snow accumulation and melt) are elevation-dependent. To that end, we combine a high-resolution gridded WG model (AWE-GEN-2d; Peleg et al., 2017) with a distributed hydrological model (Topkapi-ETH; Faticchi et al., 2015) to quantify the impacts of climate change within two mountainous catchments that are exemplary of typical mesoscale catchments in the

European Alps. We estimate the impact of climate change throughout the 21st century on a broad range of hydrological processes, such as streamflow, evapotranspiration, soil moisture, and snow water equivalent, to explore (a) the contribution of catchment-wide hydrological processes to annual and seasonal streamflow change at the outlet; (b) the propagation of changes in extreme rainfall to floods, and whether flood changes follow the climatic signal in extreme rainfall; and (c) the signal of streamflow change in many sub-catchments at different elevations, identifying the main hydrological causal components, and answering the question if the signal at the outlets reflects the spatial variability of changes across the catchments.

2. Methods

2.1. Study area and data

The Thur and Kleine Emme catchments, which represent typical mountainous sub-Alpine (non-glacierized) catchments, were chosen for this study (Fig. S-1). The river regime of both catchments is close to natural. There are no reservoirs, artificial lakes or dams in either of the catchments, nor major withdrawals for irrigation or hydropower production. In addition, the catchments are glacier free.

The Thur catchment is located in the northeastern part of Switzerland (47.4°N, 9.1°E). It is a tributary of the Rhine, with a total drainage area of 1,730 km² and an elevation range between 359 and 2434 m. The average precipitation over the catchment for the present climate is 1350 mm y⁻¹, the average annual temperature is 8.4 °C, with average streamflow at the outlet of 46.7 m³ s⁻¹ (851 mm yr⁻¹). The Kleine Emme catchment is located in central Switzerland (46.9°N, 8°E). It has a total drainage area of 477 km² and an elevation range between 430 and 2330 m. The precipitation average over the catchment for the present climate is 1650 mm y⁻¹, and the average streamflow at the outlet is 12.6 m³ s⁻¹ (833 mm yr⁻¹). Except for small cropland areas and villages, the catchments are covered mostly by natural vegetation and pastures. Both catchments have already been studied in the context of climate change impacts in the Alpine domain (Addor et al., 2014; Brunner et al., 2019; Brunner et al., 2018; Hakala et al., 2019; Keller et al., 2019; Middelkoop et al., 2001; Muelchi et al., 2020; Rössler et al., 2019).

Topographic information for both catchments was obtained by resampling a 25 m resolution digital elevation model (SwissTopo, 2002) to a 100 m × 100 m grid. Distributed land use information was obtained from the 100 m resolution Corine dataset (CLC, 2014) and soil information was extracted from the soil map of Switzerland (Bodenneignungskarte, 2012). Following Paschalis et al. (2014), the depths of the two top layers of soil for the hydrological model were set as part of the model parameterization, with the top of the groundwater layer set at a 2 m depth for zones nearby rivers and lakes, and at 5 m depth for the rest of the domain.

Meteorological data used for calibration and validation of the WG and the hydrological model (precipitation, temperature and sunshine hours) were obtained from the MeteoSwiss ground station network (SwissMetNet) at hourly resolution (Table S-1). Information on the rainfall spatial structure was derived from the MeteoSwiss C-band weather radar system (data at 2 km and 5 min, Germann et al., 2006). Hourly cloud cover data and geostrophic wind velocity at 500 hPa were obtained from the MERRA-2 reanalysis dataset (Rienecker et al., 2011). Gridded datasets for temperature (TabsD) and precipitation (RhiresD) at 2 km and daily resolution were obtained from the MeteoSwiss archive (Wüest et al., 2010; MeteoSwiss 2016). Streamflow observations (Thur at Andelfingen and Kleine Emme at Emmen) were provided by the Swiss Federal Office for the Environment.

Nine climate projections obtained from GCM-RCM model-chains from the EURO-CORDEX archive (Jacob et al., 2014; Kotlarski et al., 2014), pre-processed by MeteoSwiss (CH2018, 2018), were used to compute Factors of Change (FC, see Section 2.2) on a seasonal basis for

30-year moving windows every 10 years until the end of the century. They all follow the RCP8.5 emission scenario path and are available at a spatial resolution of 12.5 km × 12.5 km (Table S-2).

2.2. Weather generator

The AWE-GEN-2d model (Two-dimensional Advanced WEather GENERator; Peleg et al., 2017) was used to generate multiple time series at high space–time resolution (e.g., 2 km and 1 h) of the climate variables that are needed as inputs to the hydrological model. That includes precipitation, cloud cover, and near-surface air temperature at 2 m above ground (referred to as temperature here). Based on ground observations of precipitation, the model reproduces the storm arrival (wet-dry durations) as an alternating-renewal process (Peleg and Morin, 2014). Precipitation and cloud fields are simulated jointly. During wet periods, areal statistics (wet area ratio, mean areal precipitation intensity, and cloud area ratio) are calibrated to replicate the storm structure observed by weather radars, whereas during dry periods the cloud area ratio is calibrated using satellite observations, which are also used to simulate the advection of clouds and precipitation. Near-surface air temperature is simulated for a reference elevation using estimated radiation that depends on the cloud cover generated in the previous step. This value is interpolated to the whole domain through a stochastic lapse rate calibrated by ground temperature observations. The model parameters, calibration and validation processes, and advantages and limitations of the approach are discussed by Peleg et al. (2017). The AWE-GEN-2d model was successfully applied to catchments of different sizes and for various climate regions (e.g., Nyman et al., 2021; Peleg et al., 2020; Skinner et al., 2020), and its validation for the catchments used in this study is presented in Section 3.1.

AWE-GEN-2d can be used to generate ensembles of present climate simulations, when calibrated with observed meteorological data. This enables us to represent the natural climate variability, which is a fundamental component to characterize hydrological uncertainties (Faticchi et al. 2014), especially for the extremes as presented in Molnar et al. (2020) and Ruiz-Villanueva and Molnar (2020). To simulate climate variables for future periods, the model is re-parameterized based on data from RCMs and using the FC approach (e.g., Bordoy and Burlando, 2014; Faticchi et al., 2011). FC consist of the ratio or difference between climate statistics estimated from the future and present climate simulations and can be used to force the change signal in AWE-GEN-2d simulations representative of the future. This method has been previously applied in AWE-GEN-2d by Peleg et al. (2019) to produce high-resolution future climate ensembles in a nearby study area.

2.3. Hydrological model

The Topkapi-ETH model (Faticchi et al., 2015) was applied to quantify the hydrological response of the catchments to climate change. It is a fully distributed hydrological model that simulates hydrological processes in a physically explicit manner. Surface topography is represented as a regular square grid of hillslope and channel cells, while the subsurface is discretized in three layers simulating the process of infiltration and lateral flow. The top two layers represent shallow and deep soil horizons, where the lateral flow is modelled by the kinematic-wave approximation dependent on soil moisture content and soil hydraulic properties in hillslope cells (subsurface flow), and surface roughness and water depth and slope in hillslope and channel cells (overland flow and channel flow). The third layer represents the groundwater system and is modelled as a linear reservoir for flow between cells. The model simulates the lateral surface and subsurface flow between cells while considering vertical fluxes such as infiltration, exfiltration, ET, and snow and ice melt over each grid cell. The grids are connected in the surface and subsurface according to topographic gradients.

Topkapi-ETH was selected because it represents a reasonable compromise between a fully physically-based representation of

hydrological processes and computational time for large domains (>1000 km²), which allows long-term (several decades) high-resolution (sub-kilometer grid cells, hourly time steps) distributed simulation (e.g., Battista et al., 2020a; Faticchi et al., 2015). It can preserve the effects of high-resolution topography, which is an important element of hydrological simulation in complex terrain that relies on representation of overland and channel flow (e.g., Battista et al., 2020b). The model parameters, calibration and validation processes, as well as their advantages and limitations are discussed in detail by Faticchi et al. (2015). The model validation is presented in Section 3.2.

2.4. Experimental design

The numerical experiment performed in this study consisted of simulating large ensembles of climate data using AWE-GEN-2d, which were in turn used as inputs to Topkapi-ETH to obtain simulated present and future hydrological variables (Fig. 1). As a first step, both models were calibrated independently to simulate the climate and hydrological variables for the current climate conditions. AWE-GEN-2d was calibrated and validated using climate observations obtained between 1982 and 2015, following the methodologies presented by Peleg et al. (2017). The simulated time series include hourly temperature (at a 100 m resolution), precipitation (at a 2 km resolution), and catchment-averaged cloud cover. The hydrological model was calibrated and validated with streamflow at the outlet of the catchments for the period between 2000 and 2009 using observed climate forcing, following the procedures presented by Pappas et al. (2015).

In a second step, FC were computed for temperature and precipitation using the outputs of the climate models' simulations corresponding to their control (1976–2005) and future periods (2010–2089). Following Peleg et al. (2019), FC were used to re-parametrize AWE-GEN-2d to enable the simulations of continuous time series toward the end of the century. Two climate ensembles were simulated. The ensemble for the present climate consists of 15 realizations (replicates) of 30-years each. The ensemble for the future climate consists of 10 realizations of 80-years each, simulated for each of the nine climate model signals (90 trajectories in total). From this ensemble, the multi-model mean is computed as the average of the nine climate model trajectories and ten realizations. In total, the ensembles consist of 7650 years of simulations for each catchment ($30 \times 15 + 80 \times 9 \times 10$).

Third, hydrological ensembles were simulated to obtain gridded datasets (at hourly and 100 m resolution) of streamflow, snow height, snowmelt, evapotranspiration (ET), and soil moisture, and point simulations of streamflow at the river network junctions for 97 and 145 sub-catchments in the Kleine Emme and the Thur, respectively (Fig. S-2). The selected sub-catchments correspond to river reaches of Strahler order 2 or higher (Strahler, 1957) and can be nested in each other. Last, the impacts of climate change on snow depth, ET, and soil moisture, as well as on the streamflow (mean, minimum and maximum) within the catchments and at the outlet were estimated by comparing the present and future hydrological ensembles.

3. Validation of models

3.1. AWE-GEN-2d

The calibration of AWE-GEN-2d requires extensive datasets, thus often leaving few available observations for the validation process. A common assumption and procedure in the validation of WGs is that of using the same dataset necessary for the calibration, but looking at different statistics and scales (Entekhabi et al., 1989; Peleg et al., 2017). For example, comparing the simulated mean annual temperature to the gridded TabsD product on a cell-to-cell basis reveals that most grid cells in Kleine Emme (73%) show a difference between observed and simulated temperatures smaller than 1 °C (Fig. S-3, all figures related to the WG validation are presented as Supplementary Information). The same

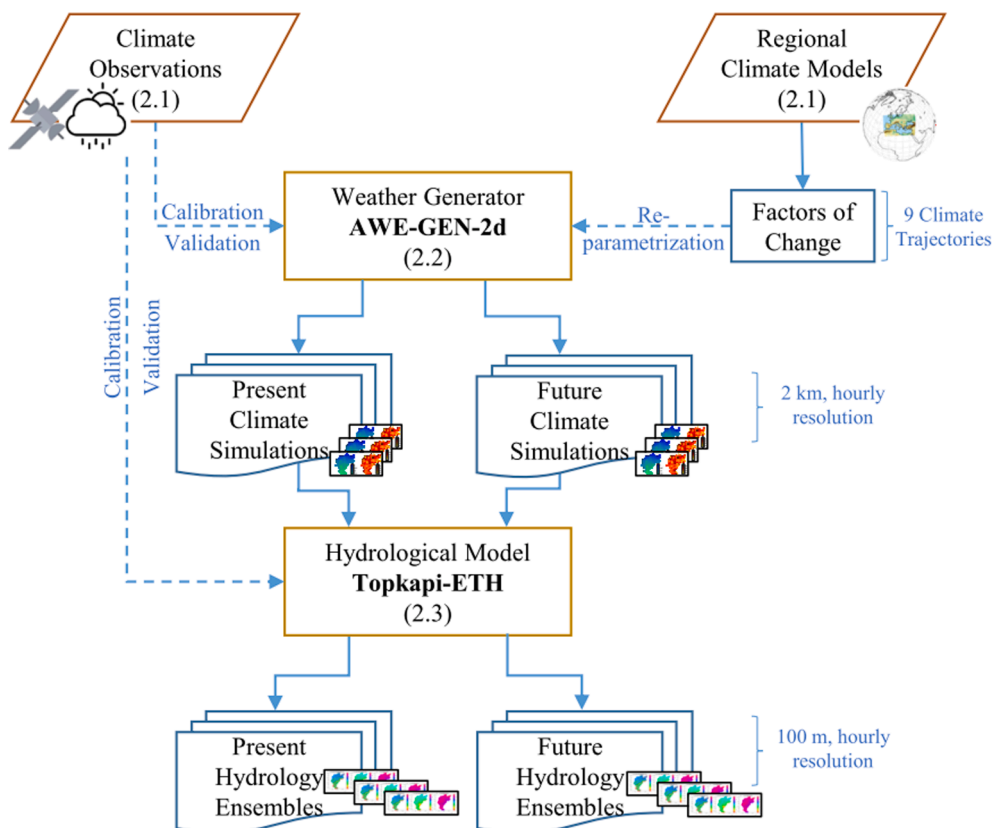


Fig. 1. A schematic representation of the numerical experiment. Shown in parenthesis are numbers of the relevant sections describing a given component of the methodology.

applies to the Thur catchment, except for the high-mountain region in the south-east where the underestimation of the temperature can reach up to 3 °C (Figure S-3). We also directly compared ground observations with the corresponding simulated grid cell in the domain and found that the WG model captures the observed temperature satisfactorily (Figure S-4): 97% of the simulated months for the Kleine Emme stations are within 1 °C of the observed mean, while in Thur the percentage drops to 67%, with the largest mean errors found in Ebnat-Kappel (EBK, 2.5 °C) and the mountain station of Säntis (SAE, 2 °C), which are however still within natural climate variability at those sites. Examining the diurnal cycle of temperature (Figure S-5), we find that the timing of the simulated maximum and minimum daily temperatures agrees well with the observed data at all stations, with the largest mean offsets in hourly temperature of 0.6 °C in Pilatus (PIL, Kleine Emme) and 1.9 °C in Ebnat-Kappel (EBK, Thur).

The spatial distribution of precipitation (Fig. S-6) is well captured in Kleine Emme. While there is a slight overestimation of the average precipitation in the WG model over the catchment in comparison to observations, the maximum overestimation is in the order of 4%, thus well within the typical measurement errors and the c. 10% expected internal climate variability for annual precipitation in this region (Fatichi et al., 2016a). In the Thur catchment, the model slightly underestimates precipitation in the north (low elevation region) and overestimates precipitation in the southern (mountainous) part, with errors in the order of 3% and well within internal climate variability. On the one hand, the model successfully reproduces the seasonal dynamics in Luzern, Napf and Aadorf-Tänikon stations, while it shows discrepancies during the spring months in Ebnat-Kappel, although observations are still within the variability range of the ensemble simulations (Fig. S-7). On the other hand, there are noticeable discrepancies for the stations Pilatus and Säntis where the model does not reproduce the recorded precipitation statistics well, although some discrepancy is expected due

to the challenge of measuring precipitation in mountaintop stations. We also evaluated AWE-GEN-2d ability to reproduce extreme precipitation at the hourly scale (Fig. S-8). The median extreme hourly precipitation computed from the simulation ensemble indicates that the model generally underestimates the extremes, but we note that (i) the observed line falls within the 5–95th ensemble range (for both Kleine Emme and Thur); and that (ii) there is considerable uncertainty in the estimates of observations as well. We also remark that AWE-GEN-2d was not calibrated to simulate sub-daily precipitation explicitly, but only on daily precipitation amounts.

3.2. Topkapi-ETH

Topkapi-ETH was validated at the hourly and monthly scales using streamflow observations at the outlet of the catchments for the 2000–2009 period. The overall agreement of the observed and simulated time series was quantified using the Nash–Sutcliffe Efficiency (NSE) index at the hourly scale, yielding values of 0.64 for Kleine Emme and 0.60 for Thur (Fig. S-9). In both catchments, the model tends to slightly underestimate the hourly peak flow values (Fig. S-10). A closer inspection of the simulations shows that the shapes of the hydrographs are reasonably similar, even if in some cases the simulation reaches the peak earlier than the observation. Notwithstanding, the reproduced peak values are within the uncertainty range of the flood series statistical model, especially for return periods lower than 30 years. At the monthly scale (Fig. S-11), Topkapi-ETH reaches NSE values of 0.76 and 0.78 for the Kleine Emme and Thur catchments, respectively, although it underestimates mean flows for October and November in the Thur catchment (up to $13.6 \text{ m}^3 \text{ s}^{-1}$).

While not perfect, we assess that the model characterizes the dynamics of streamflow correctly in terms of seasonality, the timing of the peaks, their magnitude, and hydrograph recessions. Furthermore, the

NSE values are within the range obtained using other hydrological models such as HBV, PREVAH and WaSiM for the Thur catchment (0.86, 0.81, 0.70, respectively; [Addor et al., 2014](#)), while at the same time achieving good performance at the hourly scale. For sake of consistency and to remove the biases that the weather generated forcing may introduce, the results presented in the following sections are based on the comparison of simulations using the climate ensembles (future vs. present) as input, rather than on a comparison with observed data (i.e. future vs. observed-calibrated model). This is the standard approach anytime WG forcing is used in climate change studies (e.g., [Addor et al., 2014](#); [Camici et al., 2017](#); [Fatichi et al., 2015](#)).

4. Results

We begin by presenting the results of the changes in climate at the catchment scale and how they affect the hydrological budget and the streamflow at the outlet of the catchments ([Section 4.1](#)). Then, the changes to the hydrological budget and streamflow at many sub-catchments, and their relation with elevation, are presented ([Section 4.2](#)). All of the future climate statistics represent the multi-model mean, i.e., the combination of simulations using the nine future climate trajectories considered in this study (Table S-2).

4.1. Catchment-wide impacts of climate change

The changes in temperature and precipitation are presented in [Fig. 2](#). Temperature is projected to rise progressively throughout the century until reaching an increase in the order of 4° C in the period 2080–2089 as compared to the present climate for both catchments. The increase in temperature affects all seasons with slightly higher increases in summer, and is relatively homogenous in space.

In contrast, the changes in precipitation vary in space and time. Precipitation decreases over the mountainous regions (southern areas of the catchments) and increases in the relatively low areas toward the outlets (northwest in the Thur and northeast in the Kleine Emme, [Fig. 2b, 2d](#)). Winters are projected to be wetter, particularly in the Thur catchment, and summers are projected to be drier, especially in the Kleine Emme catchment. Overall, mean precipitation is expected to decrease by 6% in Kleine Emme and increase by 5% in Thur by the end of the century.

The changes in temperature and precipitation influence changes in streamflow. Comparing the end of the century (2080–2089) and the present period, both catchments experience an increase in winter flows at the outlets by up to 40%, while summer flows at the outlets are predicted to decrease by about 20% in the Kleine Emme and by 40% in the Thur ([Fig. 3c, d](#)). The changes in streamflow at the outlet are largely following the changes in precipitation and snowmelt ([Fig. 3c, d](#)). The mean annual snow water equivalent (SWE) in the Thur decreases from 23.9 mm to 5.5 mm leading to a 48% decrease in snowmelt contribution to streamflow at the outlet on an annual average. In the Kleine Emme,

the SWE change is similar, with a decrease in the mean from 29.9 mm to 5.1 mm and a 57% decrease in snowmelt contribution to streamflow ([Fig. S-12](#)). The increase in streamflow at the outlet during winter (DJF, [Fig. 3c, d](#)) is a result of both increase in total precipitation and a shift in precipitation type from snowfall to rainfall. The latter allows precipitation to reach streamflow sooner than in the present climate (i.e., during DJF instead of MAM), as a larger portion of precipitation is not stored in the snowpack and subsequently released as snowmelt. During spring (MAM), the loss in snowmelt offsets the small increase in precipitation in both catchments. At least at the outlet, the streamflow is not affected by the changes in snowmelt during summer (JJA) and autumn (SON).

Likewise, the effect of climate change can be noticed on other hydrological components. For example, the average effective saturation of the top soil layer in the Thur remains nearly the same (25.5% to 25.7%, [Fig. 4d](#)), while a small increase is detected in Kleine Emme from 55% to 59% ([Fig. 4a](#)). The mean annual ET is projected to increase by 8% (Thur) and 10% (Kleine Emme) by the end of the century ([Fig. 4c, f](#)). The changes to ET have minor effects on the streamflow at the outlet during spring and summer, and no effect during autumn and winter ([Fig. 3c, d](#)).

In addition to the changes in mean streamflow at the outlet, we also explored the changes to extreme flows and their main driving factor – the areal extreme precipitation intensity over the catchment. Extreme hourly and daily precipitation intensities (computed from annual maxima and fitted using a Generalized Extreme Value (GEV) distribution) in both the Kleine Emme and the Thur catchments will not change considerably under climate change for the high-frequency extremes, but are projected to slightly intensify for less frequent events (up to 10% for $T = 25y$, [Fig. 5a–d](#)). However, these changes are not statistically significant as the change in the median of the computed values is minor compared to the stochastic variability obtained from analyzing multiple realizations (Table S-3). In contrast, the magnitude of flood events ([Fig. 5e–h](#)) shows, with one exception, a statistically significant decrease at the Kleine Emme (with a 5% significance level using a Mann-Whitney-Wilcoxon test, Table S-3), and particularly for the more frequent, low return-period events, whereas the decrease is not statistically significant in the Thur. This apparent contradiction, i.e. an intensification (although of small magnitude) in extreme precipitation intensities but a decrease in extreme streamflow, can be explained by changes in the antecedent soil conditions ([Fig. 4, Fig. S-13](#)), and is discussed in [Section 5](#). Additionally, a shift in the timing of the flood events is also projected; while summer will still be the season with most flood events, the frequency of floods is projected to decline during summertime and increase in the other seasons in the future ([Fig. 6](#)), following the foreseen changes in precipitation ([Fig. 2](#)).

4.2. Climate change impacts at the sub-catchment scale

At the sub-catchment scale, the impacts of climate change on streamflow vary considerably in space. To show that, we explore the

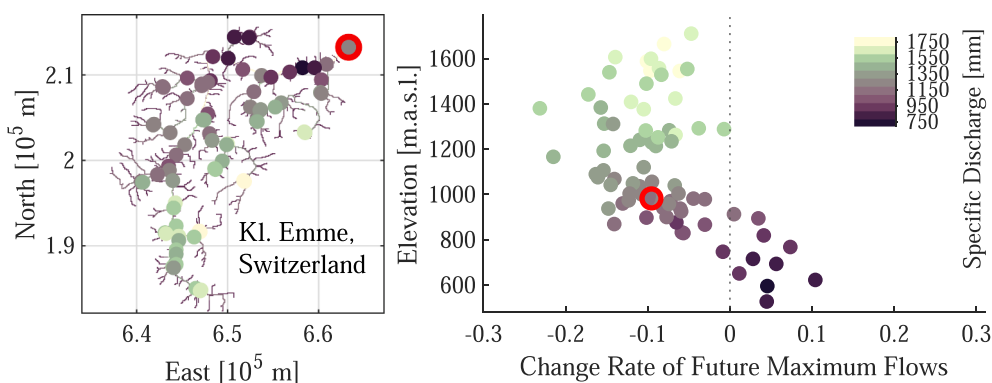


Fig. 2. Changes in precipitation (ratio of future and present climate) and temperature (difference of future and present climate) in Kleine Emme (a–d) and Thur (e–h). Panels (a, e) and (c, g) show the monthly precipitation and temperature anomalies for each future period, respectively, whereas panels (b, f) and (d, h) show the spatial distribution of the mean annual changes of the climatic variables when comparing simulations of the present climate (1976–2005) with those of the end of the century (2080–2089).

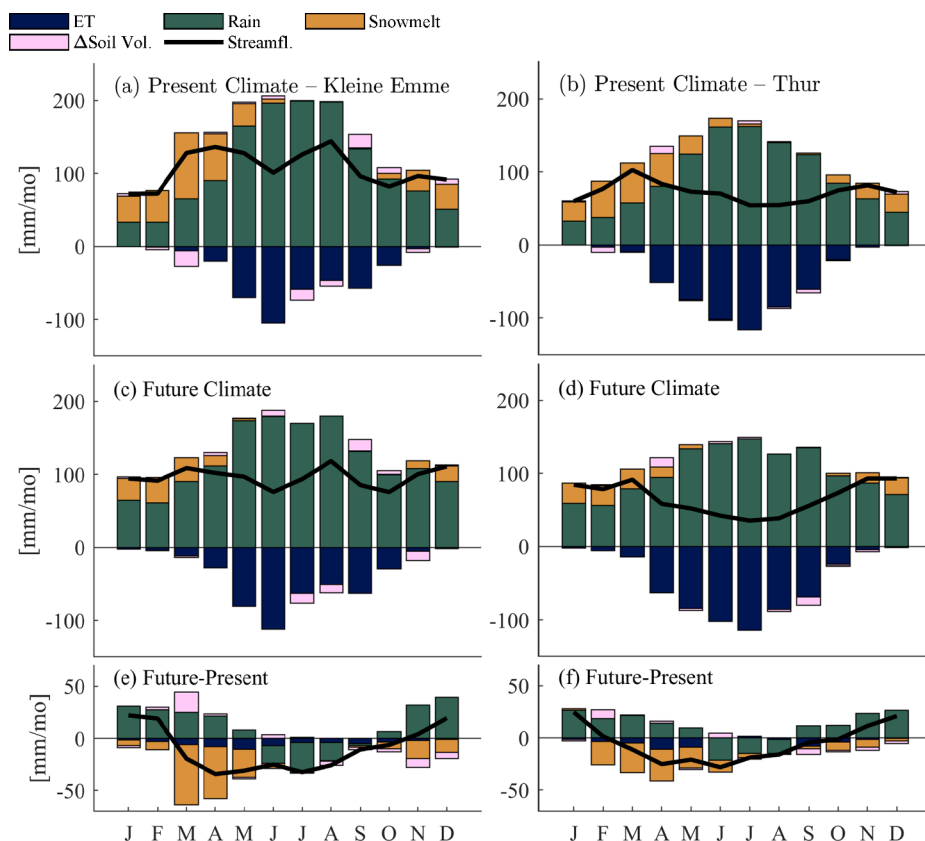


Fig. 3. Monthly streamflow (thick black line) and its hydrological components at the outlet of the Klein Emme (left) and Thur (right) river catchments for simulations of the present climate (1976–2005, a and b), of the end of the century (2080–2089, c and d), and their difference (e and f). The bars corresponding to evapotranspiration (blue) and an increase in soil water volume (pink) are depicted as negative contributions to the water balance. (For interpretation of the references to colour in this figure legend, the reader is referred to the web version of this article.)

relationship between the mean elevation of the sub-catchments and the change rate of the annual maximum hourly flow (simply termed ‘maximum’ from hereafter), mean annual flow (‘mean’), and the 7 days with the lowest flow every year (‘minimum’), computed as the difference between the future and the present streamflow divided by the present streamflow.

The changes in maximum (Fig. 7a, b) and mean flows (Fig. 7c, d) show a clear negative correlation with sub-catchment elevation: higher elevation sub-catchments show a decrease in mean and maximum streamflow, while the lower elevation sub-catchments show an increase, particularly for maximum flows, with increments up to +30% in the Thur and +10% in the Klein Emme. Changes to the minimum flows, on the other hand, have no clear relation with elevation (Fig. 7e, f). We did not find any significant correlation between the flow change rate and the size of the catchments or stream order (not shown).

Six sub-catchments within the Klein Emme catchment (as defined in Fig. S-14) that cover a range of elevations (low, mid, and high) and sizes (small and large) were selected for a further examination of the causality of the changes to the hydrological budget (Fig. 8). We found that snowmelt is a significant contributor to streamflow in sub-catchments located in high elevations during spring for the present climate, and its decrease is the main cause of decreasing flows in spring months. Sub-catchments located at lower elevation are less sensitive to changes in snowmelt. The reduction in precipitation and streamflow during summer is more noticeable higher up in the river network. The ET contribution to changes in streamflow is relatively small in all sub-catchments; however, this contribution increases in the lower elevations where ET is higher. Overall, the expected impacts of climate changes on the streamflow of lower sub-catchments in Klein Emme are almost negligible, not only at the annual scale (Fig. 7c) but at the seasonal scale as well (Fig. 9b, d). For Thur (Fig. S-15), however, changes are considerably larger at these lower elevations and mostly dictated by higher precipitation.

Moreover, we computed the first and second most important hydrological component in terms of the total volume contributed to the sub-catchment streamflow in the Klein Emme catchment in each season, for the present and end-of-the-century climates (Fig. 9). In the present climate, rainfall is the most dominant component across all seasons, excluding low sub-catchments in DJF and high sub-catchments in MAM where snowmelt is the most important contributor to streamflow. With the decreasing snowmelt by the end of the century, however, even the streamflow in these sub-catchments will be dominated by liquid precipitation. Furthermore, for many of the sub-catchments where snowmelt is currently the second most important component, ET will replace it as a relatively larger contributor by the end of the century. In summer (JJA) and autumn (SON), rainfall will remain the most important contributor throughout the catchment as the ET increase in JJA drives a decrease in overall streamflow. In SON we note that very little variation in streamflow is expected. Similar results are found for the Thur catchment (Fig. S-15).

5. Discussion

5.1. Impacts of climate change on Swiss mountainous catchments

Considering streamflow changes at the outlet for both catchments, the mean annual streamflow is projected to decrease by around 7–8% toward the end of the century (Fig. 3). For the Thur catchment, similar estimates of change were found by Jasper et al. (2004), Köplin et al. (2012), Addor et al. (2014) and Muelchi et al. (2020). These studies used different hydrological models (WaSiM-ETH; PREVAH; 3 hydrological models: HBV, PREVAH, and WaSiM; and PREVAH, respectively) and climate scenarios as inputs (GCMDAT; CH2011; CH2011; and CH2018, respectively). This points to a convergence in the estimate of the average magnitude of the change. Likewise, the above studies agree with the projected changes to streamflow at the seasonal scale, i.e., a decrease in

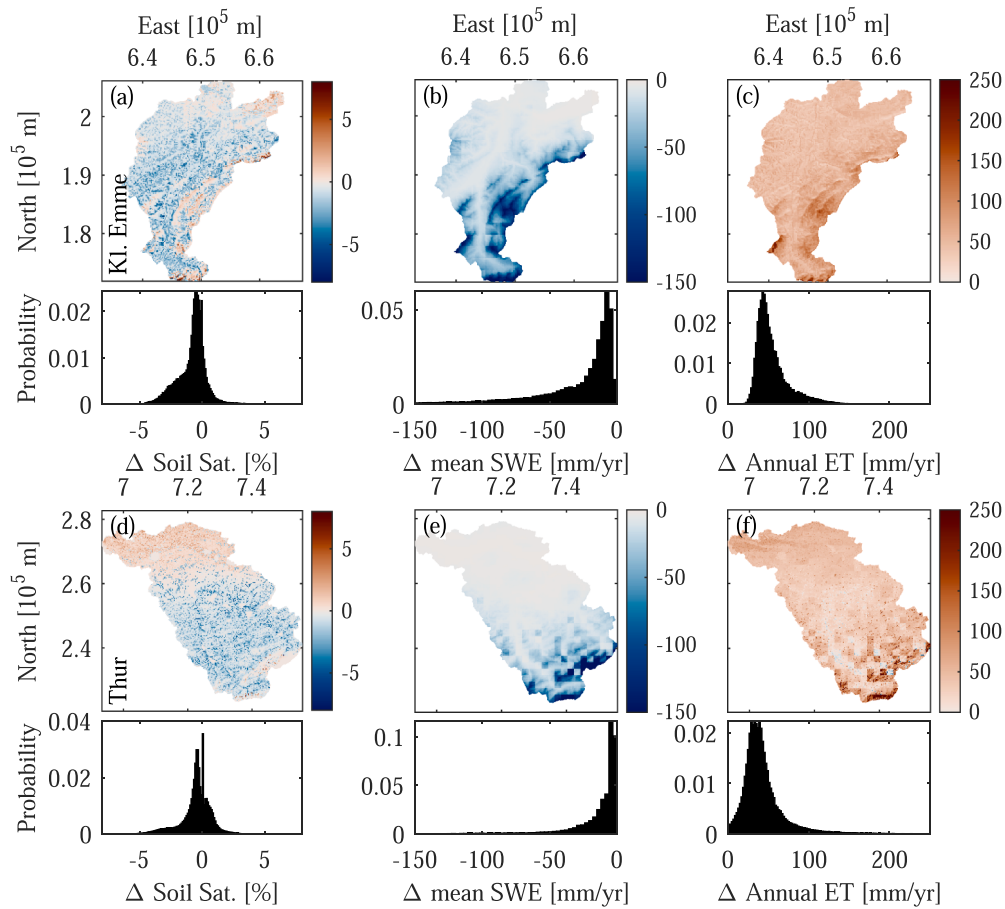


Fig. 4. Spatial distribution and histograms of the change (end-of-the-century minus present) in mean annual effective saturation (left column), snow water equivalent (middle) and evapotranspiration (right) for the Kleine Emme (a–c) and Thur (d–f) catchments.

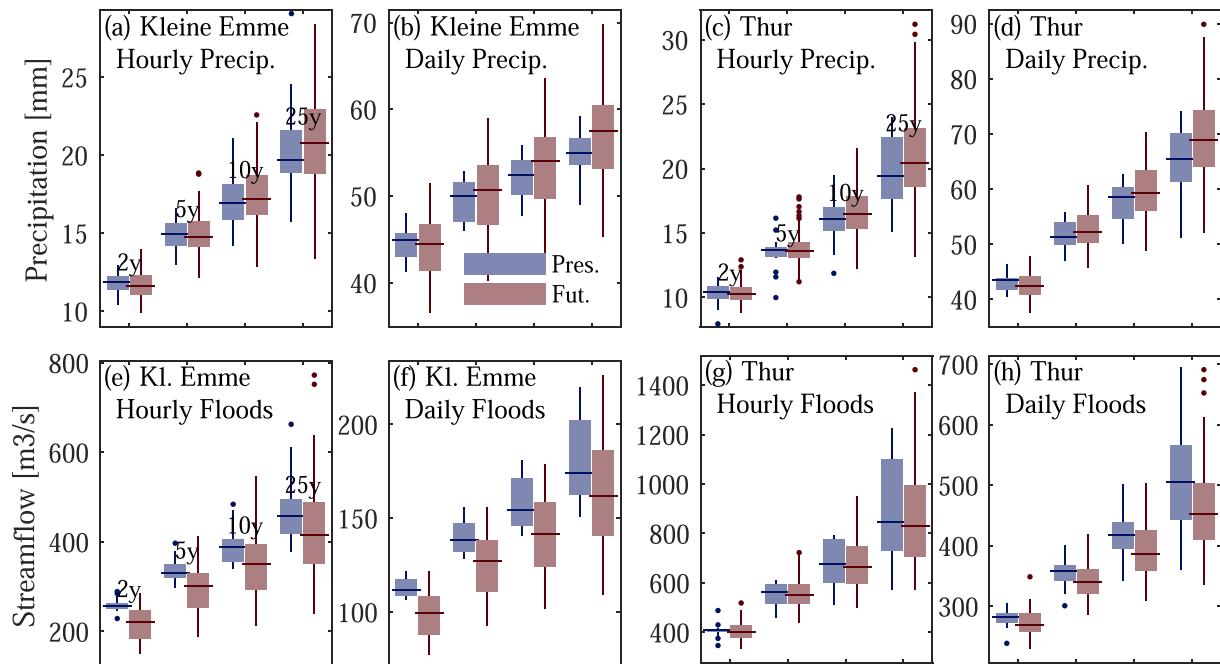


Fig. 5. Hourly and daily areal precipitation extremes (a–d) and streamflow extremes (e–h) for given return periods under present (blue) and end-of-the-century (red) climate in the Kleine Emme and Thur catchment outlets. The central lines in the box plots represent the median value computed from the simulated ensembles fitted to a GEV distribution, while the boxes represent the 25–75th percentile range emerging from the climate ensemble. (For interpretation of the references to colour in this figure legend, the reader is referred to the web version of this article.)

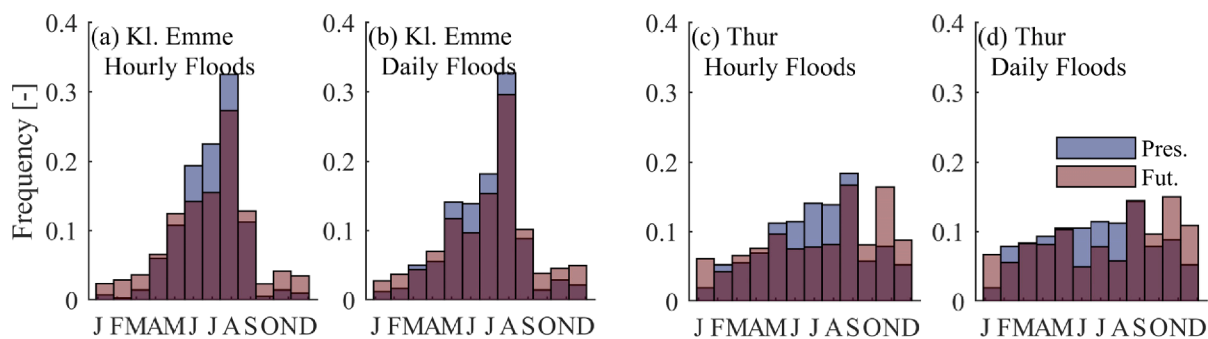


Fig. 6. Monthly frequency of the time of occurrence of hourly (a, c) and daily (b, d) annual maximum streamflow at the outlet in the Kleine Emme (a–b) and Thur (c–d) catchments simulated for present (1976–2005, blue) and for end-of-the-century (2080–2089, red) climate conditions. (For interpretation of the references to colour in this figure legend, the reader is referred to the web version of this article.)

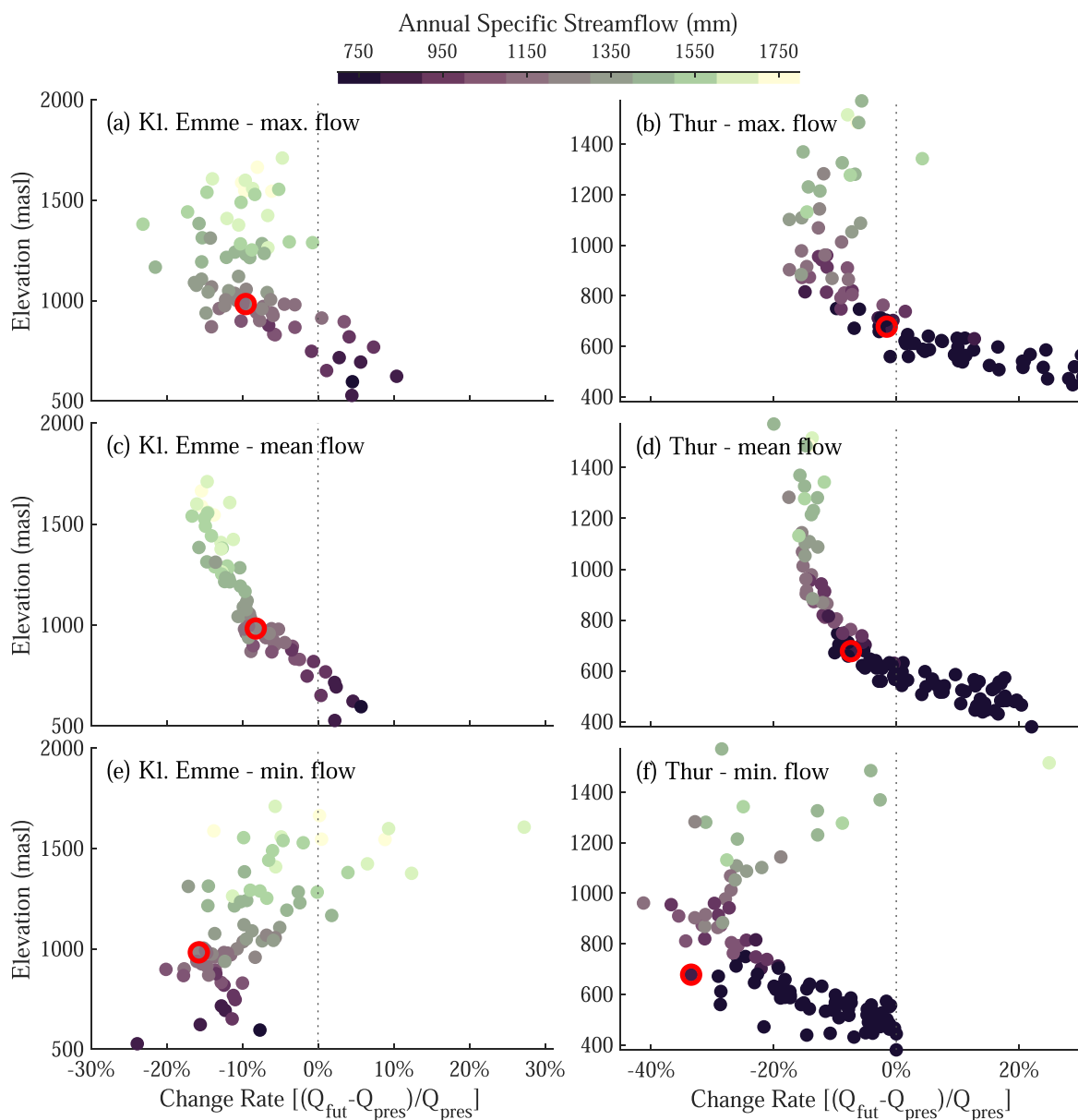


Fig. 7. Mean elevation and impacts on streamflow for 97 Kleine Emme river sub-catchments (a, c, e) and 140 Thur river sub-catchments (b, d, f). The change rates between the present climate and the end-of-the-century are computed for the maximum hourly flow (a, b), mean flow (c, d) and 7-day minimum flow (e, f). The markers in all plots are colored according to the mean specific streamflow (the ratio of streamflow to sub-catchment area) in the present climate, and the point corresponding to the outlet of the catchment is marked with a red border. (For interpretation of the references to colour in this figure legend, the reader is referred to the web version of this article.)

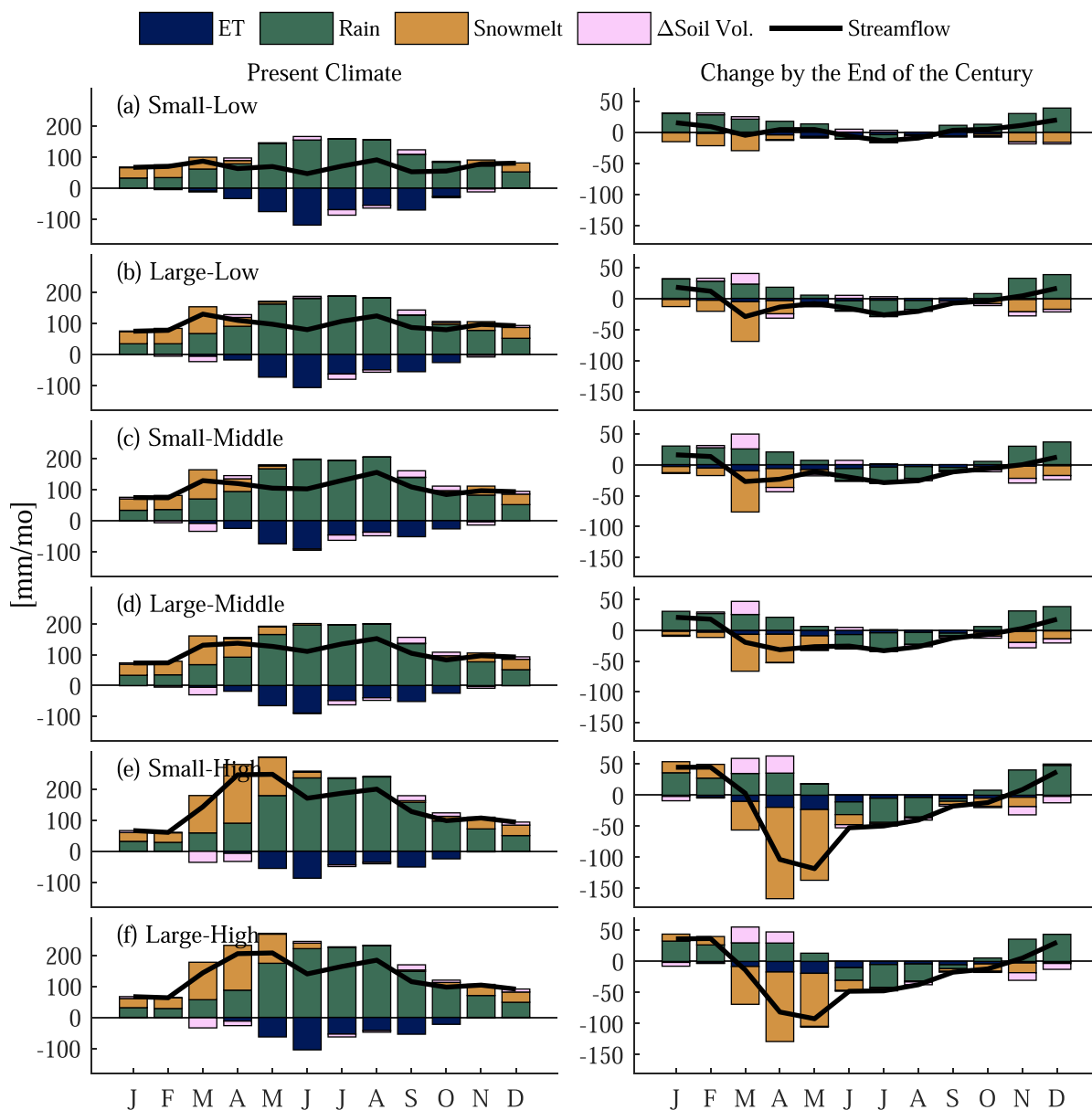


Fig. 8. Monthly streamflow (black line) and the hydrological components (bars) for six selected sub-catchments of the Kleine Emme river simulated under present climate conditions (left column), and their change towards the end of the century (right column). The bars corresponding to ET (blue) and increase in soil water volume (pink) are depicted as negative contributions to the water balance. (For interpretation of the references to colour in this figure legend, the reader is referred to the web version of this article.)

summer streamflow and an increase in winter streamflow by the end 21st century (Fig. 3). Similar degrees of change in mean annual and seasonal streamflow were reported in other European alpine catchments (Bavay et al., 2013; Etter et al., 2017; Fatichi et al., 2015; Meißl et al., 2017; Ragetti et al., 2021).

In this study, we add a new perspective on elevation-dependent changes in the sign and magnitude of streamflow at sub-catchment scales (Fig. 7). While at almost all elevations and in all seasons precipitation is found to be the key driver of the change (Fig. 9), we show that snowmelt (for sub-catchments located at high elevation) and ET (at low elevations) can also become important contributors to the changes in streamflow in a warmer climate (Fig. 8). As the changes in precipitation are a key driver, their uncertainties and impacts on the streamflow in mountainous catchments need to be better understood, and this should be investigated in more detail. For example, in our simulation of future precipitation, only the intensities were modified using FC, while the spatial and temporal structure of the precipitation process remained

unchanged, i.e. we assumed the wet periods, the temporal intermittency, and the wet area ratio to follow the same statistics as of today. Modelling these parameters in a future climate requires precipitation data outputs from climate models at a sub-daily resolution that are not commonly available in current experiments.

The projection of a decrease in snow water equivalent and its temporal shift in a future climate is in agreement with other studies in the region (Bavay et al., 2013; Etter et al., 2017; Frei et al., 2018; Jenicek et al., 2018), particularly at higher elevations (Fig. 8). Bavay et al (2013) forecast a loss of between one and two thirds of SWE by the end of the century depending on the driving climate model, which is in line with our results. Although the results agree on an increase of winter flows, they point to increases in spring as well, albeit for a domain with overall higher elevations than the study sites analysed here. Frei et al. (2018) show that snowfall will decrease dramatically by the end of the century, except during the winter months for higher elevations (above 2000 m.a.s.l.). Likewise, our results show snowfall rates at around 70% of the

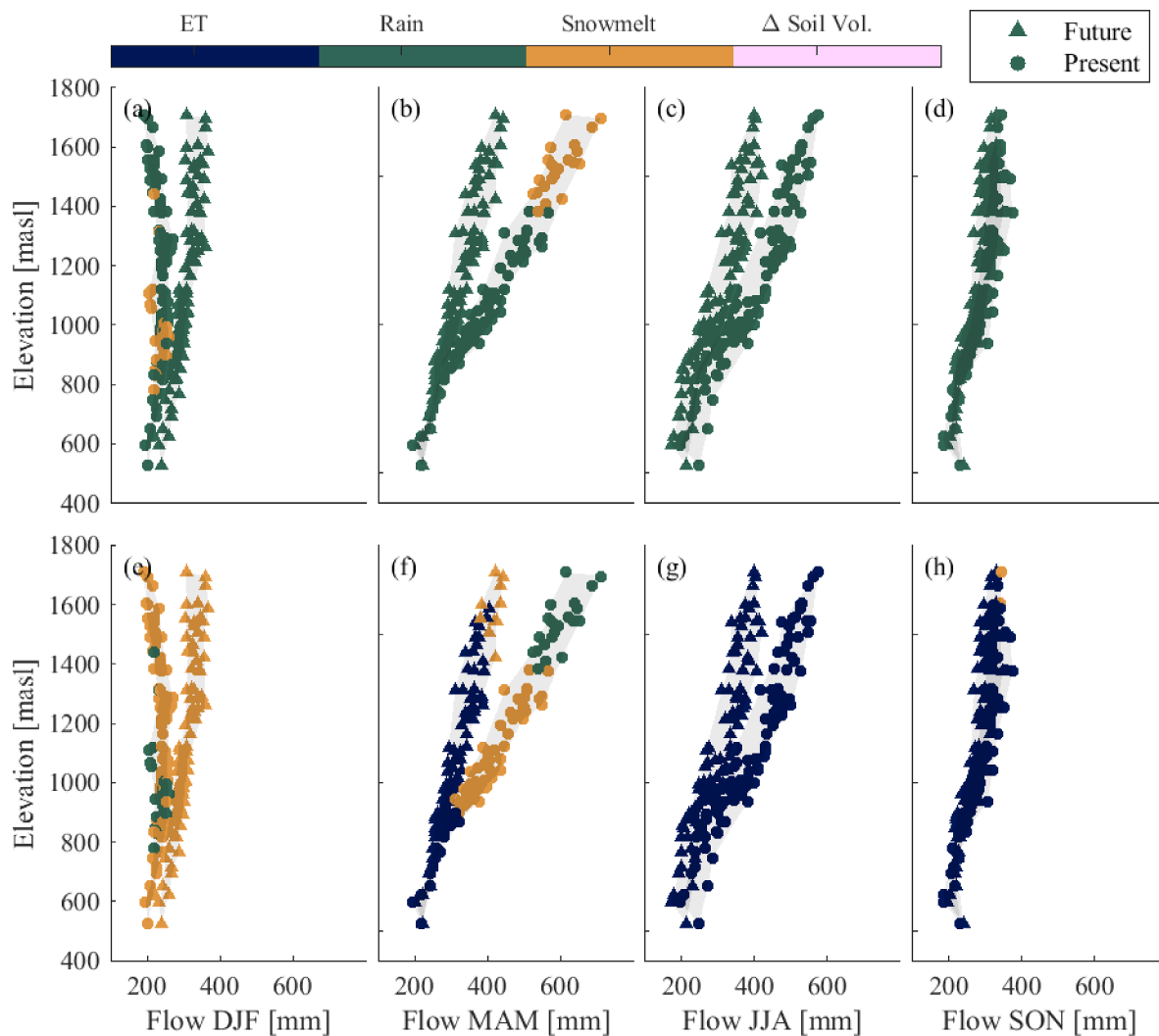


Fig. 9. First (a–d) and second (e–h) most important components contributing to the seasonal flow in the Kleine Emme river network under present (circles) and future (triangles) climate conditions. Mean seasonal specific flow is plotted as a function of mean sub-catchment elevation and colored by the components ET (evapotranspiration), Rain, Snowmelt, Δ Soil Volume (change in soil water volume).

present climate for the same months and elevations (Fig. S-16). Jenicek et al. (2018) conclude that changing SWE availability will translate into a stark decrease of low flows in the lowest catchments, but not at higher elevations, whereas our results are more ambiguous (Fig. 7). Lastly, it has to be mentioned that the presence of glaciers will certainly affect flow seasonality and especially low flow statistics in a future climate (Bavay et al., 2013), which is obviously not reflected in the results presented here for these two glacier-free catchments.

The rising temperature will cause evapotranspiration to increase all over the study catchments (Fig. 4). Mastrotheodoros et al. (2020) noted a clear correlation between ET increase and elevation simulated over the European Alps, which we observe for the Kleine Emme, but not for the Thur (Fig. S-17).

5.2. Changes to high and low flow extremes

The changes in extreme precipitation are not significant as extreme rainfall remains the same for the high-frequency return periods and increases only slightly at low-frequencies (Fig. 5, top row), yet hourly and daily streamflow extremes in our analysis are projected to slightly decrease (Fig. 5, bottom row). This apparent contradiction can largely be explained by drier antecedent soil wetness conditions prior to heavy rainfall events. Paschalis et al. (2014) used the same hydrological model

(Topkapi-ETH) and catchment (Kleine Emme) in an event-based analysis to show that drier pre-event soil moisture conditions lead to lower flood peaks on average. Indeed, in both catchments, we detect a deficit in the soil wetness before high-flow events when comparing the present and end-of-century periods (Fig. S-13). This is caused by more intense drying of the soils by ET and soil water drainage during inter-storm periods in the warm season in a future climate.

We found that the magnitudes of the annual maximum flows are projected to decrease slightly for almost all return periods at the outlets of the Thur and Kleine Emme catchments at the end of the century (Fig. 5). Our findings seem to contradict results from other studies in Switzerland which also use the CH2018 data, albeit with different hydrological models and different parameterizations, that report a projected increase in annual maximum daily streamflow toward the end of the century (Brunner et al., 2019; Molnar et al., 2020; Ruiz-Villanueva and Molnar, 2020). Nonetheless, it is worth noting that all the studies agree on the high uncertainty that accompanies such predictions. The discrepancy in the changes of the annual maximum flow magnitudes in these studies can be explained by the climatic input data used to run the hydrological models. Although the same data source was used (i.e., climate variables processed in the CH2018 project), here we further downscaled the precipitation and temperature data to obtain a higher space–time resolution using the WG. While the space–time structure of

precipitation is statistically similar to the native CH2018 data (the WG is calibrated to reproduce these statistics, see Peleg et al., 2017), it is not identical. In terms of timing, flood occurrence is foreseen to partly shift toward the cold season; nonetheless, warm-season extreme flow events, driven mostly by high-intensity rainfall events (Barton et al., 2020; Panziera et al., 2018; Panziera et al., 2015), are projected to continue to be the most frequent extreme events also in the future (Fig. 6). Another possible contributor to floods are rain-on-snow events (RoS), which may play an important role in alpine settings (Beniston & Stoffel, 2016). Although Topkapi-ETH does consider events of rainfall over snow-covered grid cells, it does so in a simplified way that does not fully account for interactions with the snowpack. A more sophisticated approach, including the distributed modelling of snowpack characteristics, could provide interesting insight into the occurrence of RoS-triggered events.

5.3. Elevation dependence of the hydrological response to climate change

The results of this study clearly show that the hydrological response to climate change in mountainous catchments at the sub-catchment scale is strongly dependent on elevation (Fig. 7). For example, we show that annual mean streamflow is foreseen to decrease by -10% (-15%) in the upper sub-catchments of the Thur (Kleine Emme), while an increase of $+15\%$ ($+5\%$) is projected in some of the lower-elevation reaches, and the estimated change at the outlet is -7% (-8%). Similarly, floods at the hourly scale are projected to decrease by up to -15% (-20%) in the upper sub-catchments, but increase up to $+30\%$ ($+10\%$) in the lowest parts of the catchment, and change only -2% (-10%) at the outlet. Faticchi et al. (2015) also examined the changes to the streamflow response with elevation, using the same hydrological model but with different climate scenarios as inputs, for a much larger Alpine catchment — the upper Rhone in Switzerland. They reported a much higher variability in the hydrological response than found here, mostly related to a much larger variability in the projected rainfall patterns. Based on the two catchments explored here and the work of Faticchi et al. (2015), we conclude that the variability of the response with elevation is strongly related to the projected rainfall patterns and the catchment size and river network connectivity.

Overall, the results highlight the need to analyze the hydrological response to climate change not only at the outlet of mountainous catchments but also within catchments. Settlements in these catchments are often located along the main river channel as well as in the sub-catchments at lower elevations connected to it. Analyzing only the response at the outlet, the risk emerging from floods in future climate can be significantly underestimated (or even the direction of change may be misrepresented). For example, in the Thur River, no change is projected to the maximum streamflow at the outlet of the catchment, while the maximum streamflow in some of the sub-catchments near the outlet is projected to increase by more than 20% (Fig. 7). This type of information is critical for urban planners, civil and environmental engineers, and policymakers that aim at planning a flood-resilient environment. This shows how the methodological framework presented in this work leads to results that emphasize the relevance of using high-resolution, distributed climatic and hydrological models for revealing important details of the hydrological response in such mountainous environments.

6. Conclusions

The impacts of climate change on mountainous catchments were studied using a high-resolution weather generator and a fully-distributed hydrological model to analyze the spatially-explicit hydrological response within two mountainous catchments in the Swiss Alps. Changes in precipitation patterns and a strong reduction in snowfall and snowmelt drive noticeable changes in streamflow at the outlet of the catchments throughout the 21st century, with decreasing summer and

increasing winter flows. In terms of streamflow extremes, we show that, despite no significant change in extreme precipitation magnitudes, maximum floods at the outlets of the catchments will decline slightly and shift in time towards the cold season. Most importantly, exploring the changes at the sub-catchment scale, we show that the mean and extreme streamflow at high-elevation sub-catchments is projected to decrease, whereas for the lower sub-catchments an increase in both mean and extreme streamflow is foreseen, in contrast with less significant changes at the catchment outlets. While rainfall was found to be the most critical component in driving the changes in streamflow, we show that snow-related processes dominate the changes at the sub-catchments located at higher elevations, while changes in ET are relevant for the changes in streamflow only for lower elevation sub-catchments. Overall, this study highlights the value of using high-resolution climatic and hydrological modelling to reveal the spatial heterogeneity of hydrological responses to a changing climate in mountainous catchments.

Declaration of Competing Interest

The authors declare that they have no known competing financial interests or personal relationships that could have appeared to influence the work reported in this paper.

Acknowledgements

This research has been funded by the Swiss Federal Office for the Environment (FOEN), grant number 15.0003.PJ/Q123-0588. We acknowledge MeteoSwiss for providing meteorological observations, the Swiss National Centre for Climate Services (NCCS) for providing climate model simulations, and FOEN for providing hydrological observations.

Appendix A. Supplementary data

Supplementary data to this article can be found online at <https://doi.org/10.1016/j.jhydrol.2021.126806>.

References

- Abegg, B., Agrawala, S., Crick, F., & de Montfalcon, A., 2007. Climate change impacts and adaptation in winter tourism. *Climate change in the European Alps: Adapting winter tourism and natural hazards management*, 25–58.
- Addor, N., Rössler, O., Köplin, N., Huss, M., Weingartner, R., Seibert, J., 2014. Robust changes and sources of uncertainty in the projected hydrological regimes of Swiss catchments. *Water Resour. Res.* 50 (10), 7541–7562. <https://doi.org/10.1002/2014WR015549>.
- Ban, N., Schmidli, J., Schär, C., 2015. Heavy precipitation in a changing climate: does short-term summer precipitation increase faster? *Geophys. Res. Lett.* 42 (4), 1165–1172. <https://doi.org/10.1002/2014GL062588>.
- Bao, J., Sherwood, S.C., Alexander, L.V., Evans, J.P., 2017. Future increases in extreme precipitation exceed observed scaling rates. *Nat. Clim. Chang.* 7 (2), 128–132. <https://doi.org/10.1038/nclimate3201>.
- Barton, Y., Sideris, I.V., Raupach, T.H., Gabella, M., Germann, U., Martius, O., 2020. A multi-year assessment of sub-hourly gridded precipitation for Switzerland based on a blended radar—rain-gauge dataset. *Int. J. Climatol.* 40 (12), 5208–5222. <https://doi.org/10.1002/joc.v40.1210.1002/joc.6514>.
- Battista, G., Molnar, P., Burlando, P., 2020a. Modelling impacts of spatially variable erosion drivers on suspended sediment dynamics. *Earth Surf. Dyn.* 8 (3), 619–635. <https://doi.org/10.5194/esurf-8-619-2020>.
- Battista, G., Schlunegger, F., Burlando, P., Molnar, P., 2020b. Modelling localized sources of sediment in mountain catchments for provenance studies. *Earth Surf. Process. Landforms* 45 (14), 3475–3487. <https://doi.org/10.1002/esp.v45.1410.1002/esp.4979>.
- Bavay, M., Grünewald, T., Lehning, M., 2013. Response of snow cover and runoff to climate change in high Alpine catchments of Eastern Switzerland. *Adv. Water Resour.* 55, 4–16. <https://doi.org/10.1016/j.advwatres.2012.12.009>.
- Beniston, M., Stoffel, M., 2016. Rain-on-snow events, floods and climate change in the Alps: events may increase with warming up to 4 °C and decrease thereafter. *Sci. Total Environ.* 571, 228–236. <https://doi.org/10.1016/j.scitotenv.2016.07.146>.
- Beniston, M., Farinotti, D., Stoffel, M., Andreassen, L.M., Coppola, E., Eckert, N., Fantini, A., Giacomini, F., Hauck, C., Huss, M., Huwald, H., Lehning, M., López-Moreno, J.L., Magnusson, J., Marty, C., Morán-Tejeda, E., Morin, S., Naaim, M., Provenzale, A., Rabatel, A., Six, D., Stötter, J., Strasser, U., Terzago, S., Vincent, C.,

2018. The European mountain cryosphere: A review of its current state, trends, and future challenges. *Cryosphere*. <https://doi.org/10.5194/tc-12-759-2018>.
- Blanc, P., Schaedler, B., 2014. Water in Switzerland—an overview. *Swiss Hydrol. Commission Rep.* 28.
- Bodeneignungskarte: 77.2 Digitale Bodeneignungskarte der Schweiz, <https://www.blw.admin.ch/blw/de/home/politik/datenmanagement/geografisches-informationsystem-gis/download-geodaten.html>, 2012.
- Bordoy, R., Burlando, P., 2014. Stochastic downscaling of climate model precipitation outputs in orographically complex regions: 2. Downscaling methodology. *Water Resour. Res.* 50 (1), 562–579. <https://doi.org/10.1002/wrcr.v50.1.1002/wrcr.20443>.
- Brunner, M.I., Sikorska, A.E., Seibert, J., 2018. Bivariate analysis of floods in climate impact assessments. *Sci. Total Environ.* 616–617, 1392–1403. <https://doi.org/10.1016/j.scitotenv.2017.10.176>.
- Brunner, M.I., Farinotti, D., Zekollari, H., Huss, M., Zappa, M., 2019. Future shifts in extreme flow regimes in Alpine regions. *Hydrol. Earth Syst. Sci.* 23, 4471–4489. <https://doi.org/10.5194/hess-23-4471-2019>.
- Bultot, F., Gellens, D., Schädler, B., Spreafico, M., 1994. Effects of climate change on snow accumulation and melting in the Broye catchment (Switzerland). *Clim. Change* 28 (4), 339–363. <https://doi.org/10.1007/BF01104078>.
- Camici, S., Brocca, L., Moramarco, T., 2017. Accuracy versus variability of climate projections for flood assessment in central Italy. *Clim. Change* 141 (2), 273–286. <https://doi.org/10.1007/s10584-016-1876-x>.
- CH2018, 2018. CH2018—Climate Scenarios for Switzerland: Technical Report. Zurich: National Centre for Climate Services.
- CLC, 2014. Corine Land Cover (CLC) map 2012, <https://land.copernicus.eu/pan-european/corine-land-cover/clc-2012>.
- Entekhabi, D., Rodriguez-Iturbe, I., Eagleson, P.S., 1989. Probabilistic representation of the temporal rainfall process by a modified Neyman-Scott Rectangular Pulses Model: parameter estimation and validation. *Water Resour. Res.* 25 (2), 295–302. <https://doi.org/10.1029/WR025i002p0295>.
- Etter, S., Addor, N., Huss, M., Finger, D., 2017. Climate change impacts on future snow, ice and rain runoff in a Swiss mountain catchment using multi-dataset calibration. *J. Hydrol. Reg. Stud.* 13, 222–239. <https://doi.org/10.1016/j.ejrh.2017.08.005>.
- Fatichi, S., Ivanov, V.Y., Caporali, E., 2011. Simulation of future climate scenarios with a weather generator. *Adv. Water Resour.* 34 (4), 448–467. <https://doi.org/10.1016/j.advwatres.2010.12.013>.
- Fatichi, S., Ivanov, V.Y., Caporali, E., 2013. Assessment of a stochastic downscaling methodology in generating an ensemble of hourly future climate time series. *Clim. Dyn.* 40 (7–8), 1841–1861. <https://doi.org/10.1007/s00382-012-1627-2>.
- Fatichi, S., Ivanov, V.Y., Paschalis, A., Peleg, N., Molnar, P., Rimkus, S., Kim, J., Burlando, P., Caporali, E., 2016a. Uncertainty partition challenges the predictability of vital details of climate change. *Earth's Futur.* 4 (5), 240–251. <https://doi.org/10.1002/efdt.2016.4.issue-510.1002/2015EF000336>.
- Fatichi, S., Rimkus, S., Burlando, P., Bordoy, R., 2014. Does internal climate variability overwhelm climate change signals in streamflow? The upper Po and Rhone basin case studies. *Sci. Total Environ.* 493, 1171–1182. <https://doi.org/10.1016/j.scitotenv.2013.12.014>.
- Fatichi, S., Rimkus, S., Burlando, P., Bordoy, R., Molnar, P., 2015. High-resolution distributed analysis of climate and anthropogenic changes on the hydrology of an Alpine catchment. *J. Hydrol.* 525, 362–382. <https://doi.org/10.1016/j.jhydrol.2015.03.036>.
- Fatichi, S., Vivoni, E.R., Ogden, F.L., Ivanov, V.Y., Mirus, B., Gochis, D., Downer, C.W., Camporese, M., Davison, J.H., Ebel, B., Jones, N., Kim, J., Mascaro, G., Niswonger, R., Restrepo, P., Rigon, R., Shen, C., Sulis, M., Tarboton, D., 2016b. An overview of current applications, challenges, and future trends in distributed process-based models in hydrology. *J. Hydrol.* 537, 45–60. <https://doi.org/10.1016/j.jhydrol.2016.03.026>.
- Fischer, A.M., Keller, D.E., Liniger, M.A., Rajczak, J., Schär, C., Appenzeller, C., 2015. Projected changes in precipitation intensity and frequency in Switzerland: a multi-model perspective. *Int. J. Climatol.* 35 (11), 3204–3219. <https://doi.org/10.1002/joc.4162>.
- Floriáncic, M.G., Berghuijs, W.R., Jonas, T., Kirchner, J.W., Molnar, P., 2020. Effects of climate anomalies on warm-season low flows in Switzerland. *Hydrol. Earth Syst. Sci.* 24 (11), 5423–5438. <https://doi.org/10.5194/hess-24-5423-2020>.
- Fowler, H.J., Blenkinsop, S., Tebaldi, C., 2007. Linking climate change modelling to impacts studies: recent advances in downscaling techniques for hydrological modelling. *Int. J. Climatol.* 27 (12), 1547–1578. <https://doi.org/10.1002/joc.1556>.
- Frei, P., Kotlarski, S., Liniger, M.A., Schär, C., 2018. Future snowfall in the Alps: projections based on the EURO-CORDEX regional climate models. *Cryosph.* 12 (1), 1–24. <https://doi.org/10.5194/tc-12-1-201810.5194/tc-12-1-2018-supplement>.
- Gariano, S.L., Guzzetti, F., 2016. Landslides in a changing climate. *Earth-Sci. Rev.* 162, 227–252. <https://doi.org/10.1016/j.earscirev.2016.08.011>.
- Germann, U., Galli, G., Boscacci, M., Bolliger, M., 2006. Radar precipitation measurement in a mountainous region. *Q. J. R. Meteorol. Soc.* 132 (618), 1669–1692. <https://doi.org/10.1256/qj.05.190>.
- Hakala, K., Addor, N., Teutschbein, C., Vis, M., Dakhloui, H., Seibert, J., 2019. Hydrological Modeling of Climate Change Impacts Intelligent parameter sampling (IntelSamp) View project Hydrological droughts in Sweden now and in the future: Hotspots of hazard, vulnerability, and risk View project Hydrological Modeling of Climate Change Impacts. DOI:10.1002/9781119300762.wsts0062.
- Hirschberg, J., Fatichi, S., Bennett, G.L., McArdell, B.W., Peleg, N., Lane, S.N., Schlunegger, F., Molnar, P., 2021. Climate change impacts on sediment yield and debris-flow activity in an alpine catchment. *J. Geophys. Res. Earth Surf.* 126 (1) <https://doi.org/10.1029/2020JF005739>.
- Jacob, D., Petersen, J., Eggert, B., Alias, A., Christensen, O.Bossing, Bouwer, L.M., Braun, A., Colette, A., Déqué, M., Georgievski, G., Georgopoulou, E., Gobiet, A., Menut, L., Nikulin, G., Haensler, A., Hempelmann, N., Jones, C., Keuler, K., Kovats, S., Kröner, N., Kotlarski, S., Kriegsmann, A., Martin, E., van Meijgaard, E., Moseley, C., Pfeifer, S., Preuschmann, S., Radermacher, C., Radtke, K., Rechid, D., Rounsevell, M., Samuelsson, P., Somot, S., Soussana, J.-F., Teichmann, C., Valentini, R., Vautard, R., Weber, B., Yiou, P., 2014. EURO-CORDEX: new high-resolution climate change projections for European impact research. *Reg. Environ. Chang.* 14 (2), 563–578. <https://doi.org/10.1007/s10113-013-0499-2>.
- Jasper, K., Calanca, P., Gyalistras, D., Fuhrer, J., 2004. Differential impacts of climate change on the hydrology of two Alpine river basins. *Clim. Res.* 26, 113–129. <https://doi.org/10.3354/cr026113>.
- Jenicek, M., Seibert, J., Staudinger, M., 2018. Modeling of future changes in seasonal snowpack and impacts on summer low flows in alpine catchments. *Water Resour. Res.* 54 (1), 538–556. <https://doi.org/10.1002/wrcr.v54.1.1002/2017WR021648>.
- Jörg-Hess, S., Griessinger, N., Zappa, M., 2015. Probabilistic forecasts of snow water equivalent and runoff in mountainous areas. *J. Hydrometeorol.* 16, 2169–2186. <https://doi.org/10.1175/JHM-D-14-0193.1>.
- Keller, D.E., Fischer, A.M., Frei, C., Liniger, M.A., Appenzeller, C., Knutti, R., 2015. Implementation and validation of a Wilks-type multi-site daily precipitation generator over a typical Alpine river catchment. *Hydrol. Earth Syst. Sci.* 19 (5), 2163–2177. <https://doi.org/10.5194/hess-19-2163-2015>.
- Keller, D.E., Fischer, A.M., Liniger, M.A., Appenzeller, C., Knutti, R., 2017. Testing a weather generator for downscaling climate change projections over Switzerland. *Int. J. Climatol.* 37 (2), 928–942. <https://doi.org/10.1002/joc.4750>.
- Keller, L., Rössler, O., Martius, O., Weingartner, R., 2019. Comparison of scenario-neutral approaches for estimation of climate change impacts on flood characteristics. *Hydrol. Process.* 33 (4), 535–550. <https://doi.org/10.1002/hyp.13341>.
- Köplin, N., Schädler, B., Viviroli, D., Weingartner, R., 2012. Relating climate change signals and physiographic catchment properties to clustered hydrological response types. *Hydrol. Earth Syst. Sci.* 16, 2267–2283. <https://doi.org/10.5194/hess-16-2267-2012>.
- Kos, A., Amann, F., Strozz, T., Delaloye, R., von Ruette, J., Springman, S., 2016. Contemporary glacier retreat triggers a rapid landslide response, Great Aletsch Glacier, Switzerland. *Geophys. Res. Lett.* 43, 12466–12474. <https://doi.org/10.1002/2016GL071708>.
- Kotlarski, S., Keuler, K., Christensen, O.B., Colette, A., Déqué, M., Gobiet, A., Goergen, K., Jacob, D., Lüthi, D., Van Meijgaard, E., Nikulin, G., Schär, C., Teichmann, C., Vautard, R., Warrach-Sagi, K., Wulfmeyer, V., 2014. Regional climate modeling on European scales: a joint standard evaluation of the EURO-CORDEX RCM ensemble. *Geosci. Model. Dev.* 7, 1297–1333. <https://doi.org/10.5194/gmd-7-1297-2014>.
- Lenderink, G., Barbero, R., Loriaux, J.M., Fowler, H.J., 2017. Super-Clausius–Clapeyron Scaling of Extreme Hourly Convective Precipitation and Its Relation to Large-Scale Atmospheric Conditions. *J. Clim.* 30 (15), 6037–6052. <https://doi.org/10.1175/JCLI-D-16-0808.1>.
- Maraun, D., Wetterhall, F., Ireson, A.M., Chandler, R.E., Kendon, E.J., Widmann, M., Brienen, S., Rust, H.W., Sauter, T., Themeßl, M., Venema, V.K.C., Chun, K.P., Goodess, C.M., Jones, R.G., Onof, C., Vrac, M., Thielen-Eich, I., 2010. Precipitation downscaling under climate change: Recent developments to bridge the gap between dynamical models and the end user. *Rev. Geophys.* 48 (3) <https://doi.org/10.1029/2009RG000314>.
- Mascaro, G., Vivoni, E.R., Méndez-Barroso, L.A., 2015. Hyperresolution hydrologic modeling in a regional watershed and its interpretation using empirical orthogonal functions. *Adv. Water Resour.* 83, 190–206. <https://doi.org/10.1016/j.advwatres.2015.05.023>.
- Mastrotheodoros, T., Pappas, C., Molnar, P., Burlando, P., Manoli, G., Parajka, J., Rigon, R., Szeeles, B., Bottazzi, M., Hadjiwoukas, P., Fatichi, S., 2020. More green and less blue water in the Alps during warmer summers. *Nat. Clim. Change* 10 (2), 155–161. <https://doi.org/10.1038/s41558-019-0676-5>.
- Mateo, C.M.R., Yamazaki, D., Kim, H., Champathong, A., Vaze, J., Oki, T., 2017. Impacts of spatial resolution and representation of flow connectivity on large-scale simulation of floods. *Hydrol. Earth Syst. Sci.* 21, 5143–5163. <https://doi.org/10.5194/hess-21-5143-2017>.
- Meißl, G., Formayer, H., Klebinder, K., Kerl, F., Schöberl, F., Geitner, C., Markart, G., Leidinger, D., Bronstert, A., 2017. Climate change effects on hydrological system conditions influencing generation of storm runoff in small Alpine catchments. *Hydrol. Process.* 31 (6), 1314–1330. <https://doi.org/10.1002/hyp.11104>.
- MeteoSwiss, 2016. Daily Precipitation (Final Analysis): RhiresD, Switzerland. [Available at <http://www.meteoswiss.admin.ch/home/search.subpage.html/en/data/product/s/2014/raeumliche-daten-niederschlag.html>].
- Middelkoop, H., Daamen, K., Gellens, D., Grabs, W., Kwadijk, J.C.J., Lang, H., Parmet, B., W.A.H., Schädler, B., Schulla, J., Wilke, K., 2001. Impact of climate change on hydrological regimes and water resources management in The Rhine Basin. *Climatic Change*.
- Milly, P.C.D., Betancourt, J., Falkenmark, M., Hirsch, R.M., Kundzewicz, Z.W., Lettenmaier, D.P., Stouffer, R.J., 2008. Climate change: Stationarity is dead: Whither water management? *Science* 319 (5863), 573–574. <https://doi.org/10.1126/science.1151915>.
- Molnar, P., Chang, Y., Yuan, Peleg, N., Moraga, S., Zappa, M., Brunner, M.I., Seibert, J., Freudiger, D., Martius, O., Mülchi, R., 2020. Future changes in floods, in: Ruiz-Villanueva, V., Molnar, P. (Eds.), Past, Current, and Future Changes in Floods in Switzerland. Hydro-CH2018 project. Commissioned by the Federal Office for the Environment (FOEN), Bern, Switzerland, pp. 51–58. DOI:10.3929/ethz-b-000462778.

- Muelchi, R., Rössler, O., Schwanbeck, J., Weingartner, R., Martius, O., 2020. Future runoff regime changes and their time of emergence for 93 catchments in Switzerland. *Hydrol. Earth Syst. Sci.* DOI:10.5194/hess-2020-516.
- Nyman, P., Yeates, P., Langhans, C., Noske, P.J., Peleg, N., Schäfer, C., Lane, P.N.J., Haydon, S., Sheridan, G.J., 2021. Probability and consequence of postfire erosion for treatability of water in an unfiltered supply system. *Water Resour. Res.* 57 <https://doi.org/10.1029/2019WR026185>.
- Panziera, L., James, C.N., Germann, U., 2015. Mesoscale organization and structure of orographic precipitation producing flash floods in the Lago Maggiore region. *Q. J. R. Meteorol. Soc.* 141 (686), 224–248. <https://doi.org/10.1002/qj.2351>.
- Panziera, L., Gabella, M., Germann, U., Martius, O., 2018. A 12-year radar-based climatology of daily and sub-daily extreme precipitation over the Swiss Alps. *Int. J. Climatol.* 38 (10), 3749–3769. <https://doi.org/10.1002/joc.2018.38.issue-1010.1002/joc.5528>.
- Pappas, C., Faticchi, S., Rimkus, S., Burlando, P., Huber, M.O., 2015. The role of local-scale heterogeneities in terrestrial ecosystem modeling. *J. Geophys. Res. Biogeosciences* 120 (2), 341–360. <https://doi.org/10.1002/2014JG002735>.
- Park, J., Onof, C., Kim, D., 2018. A hybrid stochastic rainfall model that reproduces rainfall characteristics at hourly through yearly time scale. *Hydrol. Earth Syst. Sci. Discuss.* 1–31 <https://doi.org/10.5194/hess-2018-267>.
- Paschalis, A., Faticchi, S., Molnar, P., Rimkus, S., Burlando, P., 2014. On the effects of small scale space-time variability of rainfall on basin flood response. *J. Hydrol.* 514, 313–327. <https://doi.org/10.1016/j.jhydrol.2014.04.014>.
- Peleg, N., Molnar, P., Burlando, P., Faticchi, S., 2019. Exploring stochastic climate uncertainty in space and time using a gridded hourly weather generator. *J. Hydrol.* 571, 627–641. <https://doi.org/10.1016/j.jhydrol.2019.02.010>.
- Peleg, N., Morin, E., 2014. Stochastic convective rain-field simulation using a high-resolution synoptically conditioned weather generator (HiReS-WG). *Water Resour. Res.* 50 (3), 2124–2139. <https://doi.org/10.1002/2013WR014836>.
- Peleg, N., Faticchi, S., Paschalis, A., Molnar, P., Burlando, P., 2017. An advanced stochastic weather generator for simulating 2-D high-resolution climate variables. *J. Adv. Model. Earth Syst.* 9 (3), 1595–1627. <https://doi.org/10.1002/2016MS000854>.
- Peleg, N., Marra, F., Faticchi, S., Molnar, P., Morin, E., Sharma, A., Burlando, P., 2018. Intensification of convective rain cells at warmer temperatures observed from high-resolution weather radar data. *Hydrometeorol.* 19 (4), 715–726. <https://doi.org/10.1175/JHM-D-17-0158.1>.
- Peleg, N., Sinclair, S., Faticchi, S., Burlando, P., 2020. Downscaling climate projections over large and data sparse regions: Methodological application in the Zambezi River Basin. *Int. J. Climatol.* 40 (15), 6242–6264. <https://doi.org/10.1002/joc.v40.1510.1002/joc.6578>.
- Ragetti, S., Tong, X., Zhang, G., Wang, H., Zhang, P., Stähli, M., 2021. Climate change impacts on summer flood frequencies in two mountainous catchments in China and Switzerland. *Hydrol. Res.* 52 (1), 4–25. <https://doi.org/10.2166/nh.2019.118>.
- Rienecker, M.M., Suarez, M.J., Gelaro, R., Todling, R., Bacmeister, J., Liu, E., Bosilovich, M.G., Schubert, S.D., Takacs, L., Kim, G.-K., Bloom, S., Chen, J., Collins, D., Conaty, A., da Silva, A., Gu, W., Joiner, J., Koster, R.D., Lucchesi, R., Molod, A., Owens, T., Pawson, S., Pegion, P., Redder, C.R., Reichle, R., Robertson, F. R., Ruddick, A.G., Sienkiewicz, M., Woollen, J., 2011. MERRA: NASA's Modern-Era retrospective analysis for research and applications. *J. Clim.* 24, 3624–3648. <https://doi.org/10.1175/JCLI-D-11-00015.1>.
- Rössler, O., Kotlarski, S., Fischer, A.M., Keller, D., Liniger, M., Weingartner, R., 2019. Evaluating the added value of the new Swiss climate scenarios for hydrology: an example from the Thur catchment. *Clim. Serv.* 13, 1–13. <https://doi.org/10.1016/j.cliser.2019.01.001>.
- Ruiz-Villanueva, V., Molnar, P., 2020. Past, current, and future changes in floods in Switzerland. Hydro-CH2018 project. Commissioned by the Federal Office for the Environment (FOEN), Bern, Switzerland. DOI:10.3929/ethz-b-000458556.
- Savelsberg, J., Schillinger, M., Schlecht, I., Weigt, H., 2018. The impact of climate change on Swiss hydropower. *Sustainability* 10, 2541. <https://doi.org/10.3390/su10072541>.
- Scheidt, C., Heiser, M., Kamper, S., Thaler, T., Klebinder, K., Nagl, F., Lechner, V., Markart, G., Rammer, W., Seidl, R., 2020. The influence of climate change and canopy disturbances on landslide susceptibility in headwater catchments. *Sci. Total Environ.* 742, 140588. <https://doi.org/10.1016/j.scitotenv.2020.140588>.
- Semenov, M.A., Barrow, E.M., 1997. Use of a stochastic weather generator in the development of climate change scenarios. *Clim. Change*. DOI:10.1023/A:1005342632279.
- Singer, M.B., Michaelides, K., 2017. Deciphering the expression of climate change within the Lower Colorado River basin by stochastic simulation of convective rainfall. *Environ. Res. Lett.* 12 (10), 104011. <https://doi.org/10.1088/1748-9326/aa8e50>.
- Singer, M.B., Michaelides, K., Hobley, D.E.J., 2018. STORM 1.0: A simple, flexible, and parsimonious stochastic rainfall generator for simulating climate and climate change. *Geosci. Model Dev.* 11, 3713–3726. <https://doi.org/10.5194/gmd-11-3713-2018>.
- Skinner, C.J., Peleg, N., Quinn, N., Coulthard, T.J., Molnar, P., Freer, J., 2020. The impact of different rainfall products on landscape modelling simulations. *Earth Surf. Process. Landforms* 45 (11), 2512–2523. <https://doi.org/10.1002/esp.v45.1110.1002/esp.4894>.
- Smiatek, G., Kunstmann, H., 2019. Simulating future runoff in a complex terrain alpine catchment with EURO-CORDEX data. *J. Hydrometeorol.* 20, 1925–1940. <https://doi.org/10.1175/JHM-D-18-0214.1>.
- Strahler, A.N., 1957. Quantitative analysis of watershed geomorphology. *Trans. Am. Geophys. Union* 38 (6), 913. <https://doi.org/10.1029/TR038i006p00913>.
- Swisstopo, 2002. DHM25: Das digitale Höhenmodell der Schweiz, Level 2, Bundesamt für Landestopographie, Wabern, Switzerland.
- Trzaska, S., Schnarr, E., 2014. Methods for climate change impact assessment.
- Weingartner, R., Schädler, B., Hänggi, P., 2013. Auswirkungen der Klimaänderung auf die schweizerische Wasserkraftnutzung. *Geogr. Helv.* 68, 239–248. <https://doi.org/10.5194/gh-68-239-2013>.
- Westra, S., Fowler, H.J., Evans, J.P., Alexander, L.V., Berg, P., Johnson, F., Kendon, E.J., Lenderink, G., Roberts, N.M., 2014. Future changes to the intensity and frequency of short-duration extreme rainfall. *Rev. Geophys.* 52 (3), 522–555. <https://doi.org/10.1002/2014RG000464>.
- Wheater, H.S., Chandler, R.E., Onof, C.J., Isham, V.S., Bellone, E., Yang, C., Lekkas, D., Lourmas, G., Segond, M.-L., 2005. Spatial-temporal rainfall modelling for flood risk estimation. *Stoch. Environ. Res. Risk Assess.* 19 (6), 403–416. <https://doi.org/10.1007/s00477-005-0011-8>.
- Wilks, D.S., Wilby, R.L., 1999. The weather generation game: a review of stochastic weather models. *Prog. Phys. Geogr.* 23 (3), 329–357. <https://doi.org/10.1177/030913339902300302>.
- Wüest, M., Frei, C., Altenhoff, A., Hagen, M., Litschi, M., Schär, C., 2010. A gridded hourly precipitation dataset for Switzerland using rain-gauge analysis and radar-based disaggregation. *Int. J. Climatol.* 30 (12), 1764–1775. <https://doi.org/10.1002/joc.v30.1210.1002/joc.2025>.
- Zubler, E.M., Fischer, A.M., Liniger, M.A., Schlegel, T., 2015. Auftausalzverbrauch im Klimawandel. *Fachbericht MeteoSchweiz* 253, 36.